Journal of
Materials Chemistry C

Accepted Manuscript

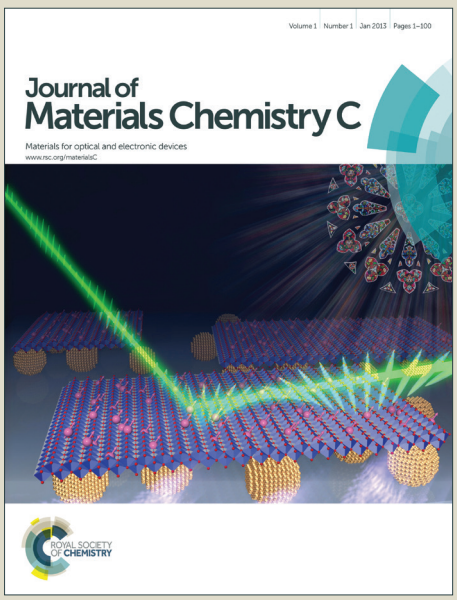

ROYAL SOCIETY OF CHEMISTRY

www.rsc.org/materialsC

Journal Name
Journal of Materials Chemistry C
Dynamic Article Links ►

Cite this: DOI: 10.1039/c0xx00000x

www.rsc.org/xxxxxx

ARTICLE TYPE

Two-step-route to Ag-Au nanoparticles grafted on Ge wafer for extra-uniform SERS substrates

Tao Wang,[a,b] Fei Hu,[a] Emmanuel Ikhile,[c] Fan Liao,[a] Yanqing Li*[a] and Mingwang Shao*[a]

Received (in XXX, XXX) Xth XXXXXXXXX 20XX, Accepted Xth XXXXXXXXX 20XX
DOI: 10.1039/b000000x

A two-step galvanic displacement reaction was employed to synthesize Ag-Au nanoparticles grafted on Ge wafer due to the different equilibrium potentials: the Ge wafer was employed to reduce silver ions and grow Ag nanoparticles first; and then it reduced gold ions and grew Au nanoparticles among the gaps of Ag nanoparticles. When they were employed as SERS substrates to detect 200 random spots, to the best of our knowledge, the lowest relative standard deviation (RSD) of less than 7% was obtained by using Rhodamine 6G (1×10^{-9} M) as probe molecules in the aqueous detection. Crystal violet solution (1×10^{-8} M) was also detected with an ultra low RSD of less than 8%. The result of the electric field distribution by the finite difference time domain simulation further explained the distinguished sensitivity and uniformity of these substrates. The high uniformity and reproducibility of this SERS substrate may benefit SERS quantitative detection in biology field in the future.

1. Introduction

Due to its excellent ability to provide unique vibrational signatures associated with chemical and structural information of the analyzed object, surface-enhanced Raman scattering (SERS) is regarded as an ideal powerful analytical tool for detecting and identifying specific targets.[1-4]

However, whether SERS can be applied as a practical application really depended on the SERS-active materials, the reproducibility of the fabrication of substrates and the uniformity of the SERS signals.[5] The latter two ensured that the observed information by SERS was reliable and accurate.

Although various techniques, such as electron beam lithography,[6] focused ion beam,[7,8] Langmuir-Blodgett assembly,[9] nanosphere lithography,[10] block copolymer template,[11] and oblique angle deposition,[12] have been developed for fabricating the high-performance SERS-active substrates, some disadvantages still need to be overcome: (1) the fabrication process was often complex and time-consuming; (2) the used surfactants or polymers would unfavorably affect the SERS detection; (3) the fabrication of SERS substrates with a large area was difficult; (4) some complex and expensive instruments were required in the fabrication process, which would restrict the popularity of these substrates.

Hence, it was highly desirable to prepare the high-performance SERS-active substrates by a green, time-saving and high-throughput method. Galvanic displacement, without the need of reducing agents and external power sources,[13,14] has been widely applied to fabricate SERS substrates.

In this paper, a two-step galvanic replacement method was proposed to directly fabricate SERS substrates based on Ag-Au nanoparticles (NPs) grown on the Ge wafer. The method was green, time-saving and low-cost. Only three ingredients, $AgNO_3$, germanium, and $HAuCl_4$ were required in the fabrication process. The absence of organic surfactant molecules in the reaction solution provided a clean environment to grow Ag-Au NPs. Finite difference time domain (FDTD) method was employed to calculate the near-field distribution on the surface of our proposed structures. Except the remarkable SERS activity, the as-prepared SERS substrates also showed the outstanding relative standard deviation (RSD) of less than 7% for Rhodamine 6G (R6G) (1×10^{-9} M) and less than 8% for crystal violet (CV) (1×10^{-8} M) in the aqueous detection. To the best of our knowledge, the value of RSD is the lowest one, demonstrating the high uniformity, sensitivity and reproducibility of the SERS substrates.

2. Experimental section

2.1 Synthesis and characterization

All chemical reagents were of analytical grade, which were purchased from Shanghai Chemical Company and used without further purification. The water used was doubly distilled water. Ge (100) wafers (*n* type, 0.01 Ω·cm) with a diameter of 50 mm and a thickness of 0.5 mm were purchased from Hefei Kejing Materials S2 Technology Co., Ltd (China).

The Ge wafer was cleaned following the previously reported process.[15] After dried with nitrogen, the Ge wafer was immediately immersed in 300 mL 1×10^{-4} M $AgNO_3$ solution and $HAuCl_4$ solution for 10 and 1 min, respectively. Between each immersion process, the Ge wafer was taken out and rinsed with doubly distilled water and methanol sequentially and dried with nitrogen gas. Finally, the Ge wafer grown with Ag-Au NPs was obtained.

The morphologies of Ag-Au NPs formed on the Ge wafer were performed on a FEI-quanta 200F SEM with acceleration voltage

of 30 kV. TEM and elemental mapping by Energy-dispersive X-ray spectrometry (EDS) analysis were performed by a FEI Tecnai F20 transmission electron microscope with an accelerating voltage of 200 kV. The ultraviolet-visible (UV-vis) absorption spectrum was recorded by a Thermo Scientific Evolution 220 Diode Array Spectrophotometer.

2.2 Theoretical calculations

In order to model theoretically the uniform plasmon coupling in the two systems, 3D-FDTD simulations were performed with FDTD Solutions from Lumerical Solutions, Inc. (Vancouver, Canada). A frequency-domain field profile monitor was used to record the electromagnetic field over the simulation region.

Figure S1 clearly shows the FDTD simulation conditions. The simulated SERS substrates were constructed of Ag or Ag-Au NP array with cubic arrangement in the *x-y* plane (Figure S1 left) and the metal NP array was placed on the top of Ge wafer in the *x-z* plane. The diameter of Ag NPs was 50 nm with the interparticle distance of 25 nm. The Au NPs with diameter of 10 nm were located in the free area among the Ag NPs with interparticle distance of 7.5 nm, as shown in Figure S1 (right).

Periodic boundary conditions were applied to the *x*- and *y*-directions to describe an infinite array, and perfectly matched layers (PML) were set to the *z*-boundaries as a boundary condition. A *p*-polarized 633 nm plane wave was placed above the system and polarized to the *x*-axis. The experimental value of Palik[16] was used for the dielectric constant of Ag, Au and Ge.

The mesh size used in the calculations was 0.5 nm × 0.5 nm × 0.5 nm. The simulation time was set at 500 fs, ensuring the fields to decay completely before termination of the simulation. The electric field intensity distribution was reported as the square of the electric field ($|E/E_0|^2$).

2.3 Raman microscopy

An HR 800 Raman spectroscopy (J Y, France) equipped with a synapse CCD detector and a confocal Olympus microscope was used to collect Raman spectra. SERS experiments were conducted in the line-mapping mode and 1 μm increment using R6G aqueous solution as model molecules. The spectrograph used 600 g/mm gratings. SERS spectra were collected at LMPlanFl 50 × objective Lens (lens with the long focal length) with a numerical aperture of 0.50 and the accumulation time of 1 s.

In order to reduce the influence of surface-enhanced resonance Raman scattering, a 633 nm He-Ne laser was employed in all the Raman detections.

3. Results and discussion

3.1 Characterization of Ag-Au NPs on Ge wafer

The morphology of the products at different steps was investigated by scanning electron microscope (SEM). Figure 1a is the low magnification image that reveals a large scale Ag NPs on a Ge wafer, which is the product after silver ions were reduced by Ge wafer. And the high magnification one (Figure 1b) shows that the average diameter of Ag NPs is 50 nm. After the second step of reduction, the gold ions were reduced and grown on Ge wafer. Figures 1c and 1d show the low and large magnification images of Ag-Au NPs on a Ge wafer. The distribution of Au and Ag NPs is still uniform. It is clearly shown in Figure 1d that Au NPs are much smaller than Ag NPs with an average diameter of 10 nm and grow among the gaps of Ag NPs. TEM image and the corresponding EDS mapping of Ag and Au nanoparticles grown on the Ge wafer are shown in Figures 1e and 1f. It is noted that small particles around the large one are Au, and the large particle is composed of Ag and Au elements, confirming that the Ag nanoparticles reacted with $HAuCl_4$ to form AgAu alloy during the reaction process.

Due to the short reaction time, the morphology change of Ag nanoparticles is very small. Through the EDS spectra analysis of the large nanoparticle (Figure S2), the content of Au is about 13.66 At%. The large particles are simplified to be Ag nanoparticles in the FDTD simulation.

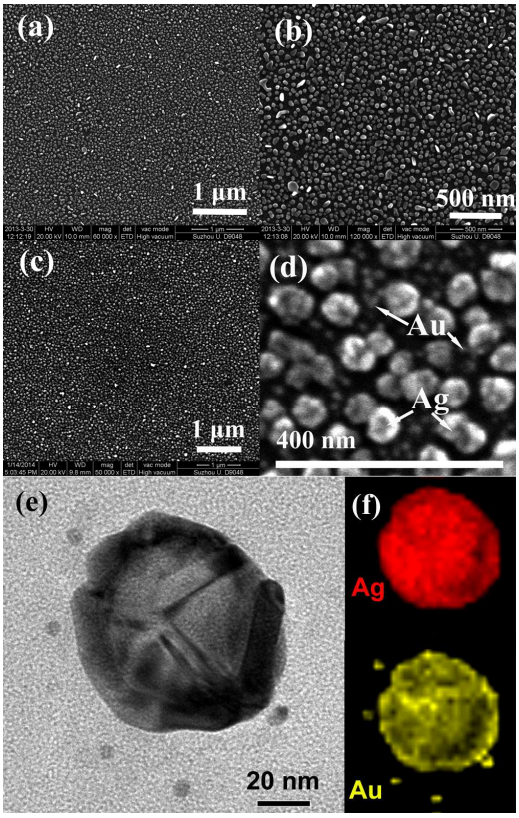

Figure 1. The SEM images of Ag NPs grown on Ge wafer in (a) low magnification and (b) high magnification; the Ag-Au NPs grown on Ge wafer in (c) low magnification and (d) high magnification; (e) TEM image and (f) EDS mapping of Ag and Au nanoparticles on the Ge wafer.

The formation of Ag-Au NPs on Ge wafer is illustrated in Figure 2: contacting the Ge wafer with $AgNO_3$ solution, Ag^+ ions were immediately reduced, resulting in the formation of small Ag nanocrystals. Once the nuclei are formed and the surface electrons are expended, Ag^+ ions continue to be reduced by electrons from Ge because the equilibrium potential of Ag^+/Ag couple (>4.885 eV for $AgNO_3$ solutions with concentrations higher than 1×10^{-7} M) is lower than the valence band of Ge (with band edge of 4.0 eV) (Figure 2a) and make Ag nuclei grow larger. The Ge with loss of electrons react with water to form GeO_2 (Figure 2b). This galvanic replacement resulted in the Ge wafer grown with Ag NPs.

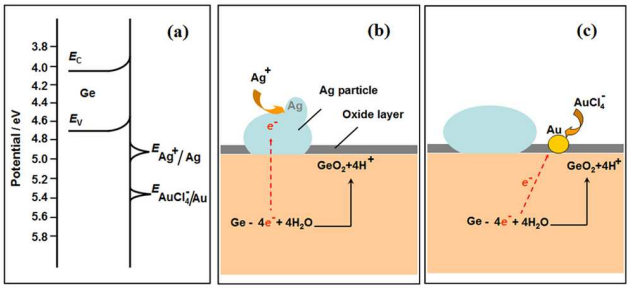

Figure 2. Schematic of the formation process of Ag-Au NPs grown on the Ge wafer.

When the Ge wafer grown with Ag NPs is immersed in $HAuCl_4$ solution, the potential of $AuCl_4^-$/Au couple (>5.364 eV for $HAuCl_4^-$ solution with concentrations higher than 1×10^{-7} M) is lower than the valence band of Ge as mentioned above, resulting in the formation of Au NPs. It should be pointed out that the potential of $AuCl_4^-$/Au couple is lower than that of Ag^+/Ag, which means that $AuCl_4^-$ ions may also be reduced by Ag, although its reducing rate is slower than that by Ge. Therefore, the reaction time is an important parameter. If we controlled the reaction time properly in the second step, Au NPs might grow on Ge wafers prior to on Ag NPs (Figure 2c).

A red shift of the peak from about 385 to 435 nm has been observed from the UV-vis spectrum of the nanoparticles (Figure S3) due to the formation of AgAu alloy. There is no obvious peak of Au nanoparticles, which may on account of the low content. The result is consistent with the EDS analysis.

3.2 SERS of Ag-Au NPs on Ge wafer

In order to get a clear prospect, FDTD was employed to simulate the SERS intensity. FDTD is a powerful numerical analysis technique for modeling computational electrodynamics.[17,18]

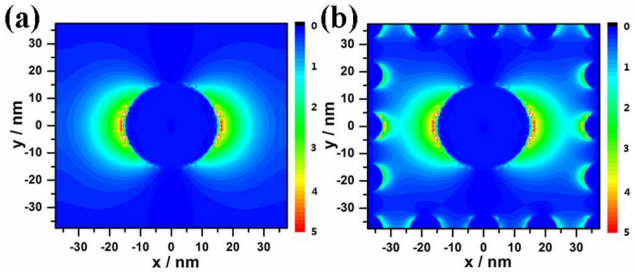

Figure 3. Electric field intensity ($\langle |E|^2 \rangle$) distributions of (a) Ag NPs and (b) Ag-Au NPs grown on Ge wafer obtained from 3D FDTD calculations at wavelength of 633nm at z = 5 nm.

The square of the electric field ($|E/E_0|^2$) in *x*-*y* plane monitor with fixed *z* value of 5 nm was reported: Figure 3a is for Ag NP array and Figure 3b for Ag-Au NP one. The detailed simulation model and theoretical calculations are in experimental section and Supporting Materials. The electric field in Figure 3a was only focused on the nearby of the Ag NP and nearly zero in the rest area, while that in Figure 3b was distributed between Ag and Au NPs, as well as the vicinages of Ag and Ag NPs. Therefore, the well-distributed electric field ($|E/E_0|^2$) of Ag-Au NP array makes it a better choice to exhibit uniform SERS activity.

In order to evaluate the SERS performance of the substrate, Raman spectra were collected using R6G as the probe molecule for its well-established vibrational features.

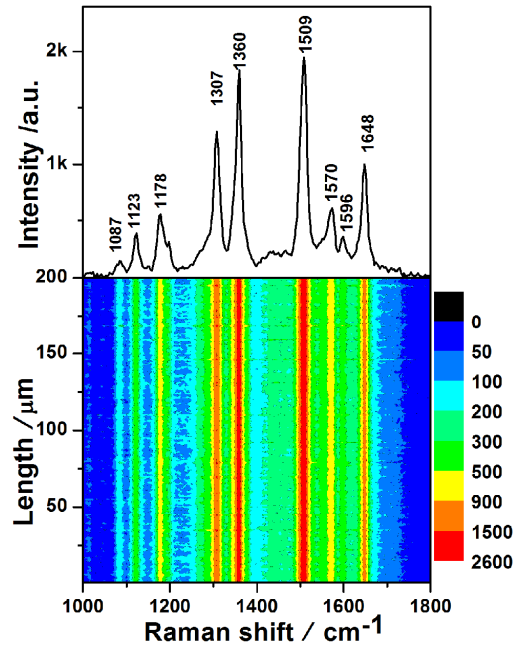

Figure 4. The Raman spectrum of R6G aqueous solution (1×10^{-9} M) on the as-prepared Ag-Au NPs/Ge substrate (upper part), and the SERS contour (lower part).

SERS measurements were conducted as follows. The Ge wafer grown with Ag-Au NPs was cut into small pieces with the size of 0.5×0.5 cm^2, and then placed in a quartz cell of 150 μL with a quartz window. The cell was filled up with 1×10^{-9} M R6G aqueous solution, and the distance between the Ge wafer and this quartz window is about 0.5 mm. In the process of Raman detection, the laser was focused on the Ag-Au NPs through the quartz window.

From the upper part of Figure 4, the remarkable SERS activity of the Ag-Au NP substrate was exhibited. The main peaks of R6G's characteristic vibrations in SERS, the strongest bands of carbon skeleton stretching modes at 1360, 1509, 1570, 1648 cm^{-1}, are similar to the normal solution Raman spectrum of R6G in Figure S4.

Another critical point shown in the lower part of Figure 4 is the exceptional uniformity of the substrate. The SERS contour was plotted after the line mapping which was measured spot-to-spot at 1×10^{-9} M R6G aqueous solution. In all the 200 spots, each spot exhibited a powerful capability of enhancing Raman signals of the R6G molecules.

To further semi-quantitatively evaluate the uniformity of these SERS signals, the RSD of the dominant characteristic peaks' intensity was calculated. The values of RSD of vibrations at 1307, 1360, 1509, and 1648 cm^{-1} (Figure 5) are 6.86%, 6.48%, 6.36%, and 6.54%, respectively. All the RSD values of the four characteristic peaks are less than 7%, which further demonstrated that the as-prepared substrate was high uniformity and suitable for a highly sensitive SERS substrate.[19,20] The log-normal distribution of R6G Raman intensities indicated that there is a large coverage of SERS hotspots in the scanned area (Figure

S5).[21] Moreover, the narrow distribution of peaks further confirmed the uniformity of SERS substrate. To quantitatively demonstrate the enhancement, the peak at 1509 cm^{-1} was used to calculate the enhancement factor (EF) using equation:[22]

$$EF=\frac{I_{SERS}N_0}{I_0N_{SERS}}$$

where N_0 and I_0 are the number of R6G molecules and intensity for regular Raman measurement with 0.01M R6G solution, respectively; and N_{SERS} and I_{SERS} are the number of R6G molecules and peak intensity for the SERS measurement, respectively. EF was calculated as 3.8×10^7. The detailed calculation is shown in Supporting Materials.

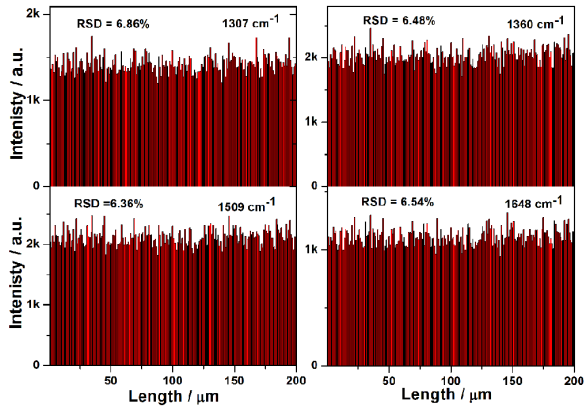

Figure 5. The intensities of the main Raman vibrations of R6G aqueous solution (1×10^{-9} M) in 200 spots SERS line-scan spectra collected on the as-prepared Ag-Au NPs/Ge substrate.

The fabulous enhancement of this SERS substrate may be the result of co-actions of the following effects: first, the surface of Ag-Au NPs was clean, which increases the surface area to adsorb more target molecules. Meanwhile, the flat Ge wafer is beneficial to the uniformity of Raman signals. Secondly, large electromagnetic field coupling at the junctions of the NPs is beneficial to excellent activity of SERS substrate. There were about 360 Ag-Au NPs in a square micrometer area, calculated from the SEM image in Figure 1c. The diameter of the laser was calculated to be 1.55 μm, according to the formula:[23]

$$D = 1.22\,\lambda/\,N_A$$

where λ is the wavelength of laser used and N_A is the numerical aperture of the objective. Finally, the laser spot covered more than 678 Ag-Au NPs ($\pi \times (1.55/2)^2 \times 360 = 678$), which ensured the large electromagnetic field coupling.

The substrate was also used to detect 1×10^{-8} M CV aqueous solution. The SERS spectrum from the CV (Figure 6, upper part) is in good agreement with literature.[24] The SERS contour (Figure 7, lower part) was obtained from the line mapping conducted spot-to-spot on the substrate in the 1×10^{-8} M CV aqueous solution. For all the 200 spots, each spot exhibits strong SERS signals. The values of RSD of vibrations at 1181, 1398, 1544, and 1628 cm^{-1} (Figure 7) are 7.50%, 7.60%, 6.97%, and 7.43%, respectively, only slightly higher than that of R6G, further demonstrating the excellent enhancement effect and high uniformity of the substrate. As is shown in Figure S6, the Raman intensities of CV also show a log-normal distribution, further indicating that there is a large coverage of SERS hotspots in the scanned area. In addition, the width of their distribution is almost identical to that in the Raman spectra of R6G, demonstrating the good reproducibility of the SERS substrate.

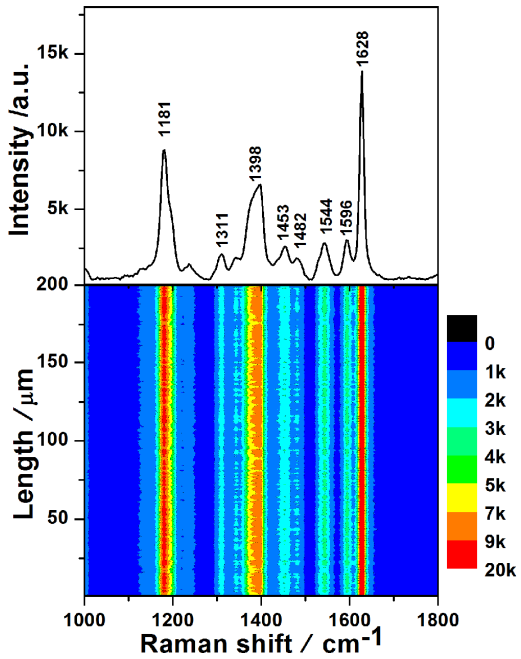

Figure 6. The Raman spectrum of CV aqueous solution (at 1×10^{-8} M) on the as-prepared Ag-Au NPs/Ge substrate (upper part), and the SERS contour (lower part).

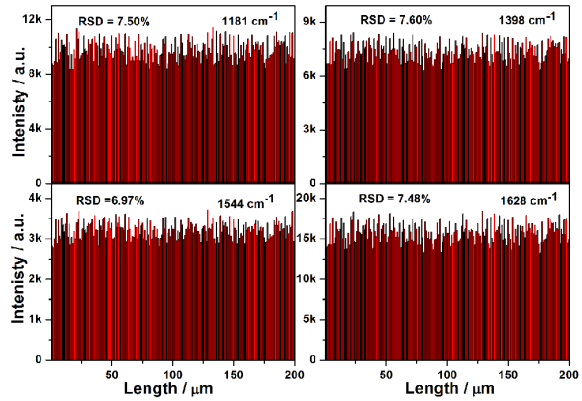

Figure 7. The intensities of the main Raman vibrations of CV aqueous solution (at 1×10^{-8} M) in the 200 spots SERS line-scan spectra collected on the as-prepared Ag-Au NPs/Ge substrate.

It is worth mention that all the measurements of Raman spectra were conducted in the aqueous solution. It helps to obtain high uniformity and reproducibility of signals and get the real structure information of molecular in solution. This is very beneficial to the research on the reaction mechanism *in situ* in solution through the Raman measurement. The as-grown Ag-Au structures have chemically clean surfaces due to the absence of surfactants or coordinating molecules involved in the synthesis, which is beneficial to attachment of interesting molecules on their surfaces for various applications, such as plasmonic enhanced photophysical/photochemical processes and surface enhanced

spectroscopies.[25] Although the Ag-Au NPs substrate exhibits no more excellent enhancement effect than Ag/Ge substrate in the SERS measurement, it shows higher uniformity (RSD is less than 7%) than the Ag/Ge substrate, in which the values of RSD are less than 11%.[26]

4. Conclusions

In summary, a large-area SERS substrate with high-performance has been fabricated via two-step galvanic displacement. The preparation process is green, time-saving and low-cost, in which only silver nitrate, germanium and $HAuCl_4$ are required. The SERS signals collected on the substrate in the dilute R6G and CV solution showed large enhancement and high sensitivity for Raman detection, which also confirmed by the electric field distribution through FDTD simulation. The spot-to-spot Raman collections of 200 spots in R6G and CV solution showed excellent detection reproducibility and the values of RSD are less than 7% and 8% of the major vibrations, respectively. We believe that this large-area SERS substrate with high sensitivity and excellent reproducibility is promising in chemical and biological detections and the researches on the mechanisms of reactions *in situ* or in solutions.

The project was supported by the National Basic Research Program of China (973 Program) (Grant No. 2012CB932903), Jiangsu Key Laboratory for Carbon-based Functional Materials and Devices & Collaborative Innovation Center of Suzhou Nano Science and Technology, Innovative Research Teams of Jiangsu Higher Education Institutions, the Priority Academic Program Development of Jiangsu Higher Education Institutions, and the Natural Science Foundation of Universities of Anhui Province (KJ2013B126).

Notes and references

[a]*Institute of Functional Nano & Soft Materials (FUNSOM), Soochow University, Suzhou 215123, P. R. China;*
[b]*School of Chemistry and Chemical Engineering, Provincial Key Laboratory of Functional Coordination Compounds and Nanomaterials, Anqing Normal University, Anqing, Anhui 246001, P.R. China*
[c]*Department of Chemical Engineering, University of Waterloo, Waterloo, Ontario, Canada N2L 3G1*
Fax: +86 512 65882846; Tel: +86 512 65880953
E-mail: mwshao@suda.edu.cn (MW Shao); yqli@suda.edu.cn (YQ Li)

† Electronic Supplementary Information (ESI) available: [FDTD simulations, normal Raman spectrum of R6G, histograms of normalized Raman intensities of R6G and CV]. See DOI: 10.1039/b000000x/

1 S. Schlucker, *Angew. Chem. Int. Ed.*, 2014, **53**, 4756.
2 N. P. W. Pieczonka and R. F. Aroca, *Chem. Soc. Rev.*, 2008, **37**, 946.
3 D. Graham, *Angew. Chem. Int. Ed.*, 2010, **49**, 9325.
4 X. H. Tang, W. Y. Cai, L. B. Yang and J. H. Liu, *Nanoscale*, 2014, **6**, 8612.
5 X. M. Lin, Y. Cui, Y. H. Xu, B. Ren and Z. Q. Tian, *Anal. Bioanal. Chem.*, 2009, **394**, 1729.
6 S. M. Wells, S. D. Retterer, J. M. Oran and M. J. Sepaniak, *ACS Nano*, 2009, **3**, 3845.
7 A. Ahmed and R. Gordon, *Nano Lett.*, 2011, **11**, 1800.
8 K. Sivashanmugan, J. D. Liao, J. W. You and C. L. Wu, *Sensors Actuat. B-Chem.*, 2013, **181**, 361.
9 J. Paczesny, A. Kamińska, W. Adamkiewicz, K. Winkler, K. Sozanski, M. Wadowska, I. Dziecielewski and R. Holyst, *Chem. Mater.*, 2012, **24**, 3667.
10 M. Kahraman, P. Daggumati, O. Kurtulus, E. Seker and S. Wachsmann-Hogiu, *Sci. Rep.*, 2013, **3**, 3396.
11 Y. Wang, M. Becker, L. Wang, J. Liu, R. Scholz, J. Peng, U. Goesele, S. Christiansen, D. H. Kim and M. Steinhart, *Nano Lett.*, 2009, **9**, 2384.
12 Y. J. Liu, H. Y. Chu and Y. P. Zhao, *J. Phys. Chem. C,* 2010, **114**, 8176.
13 C. Carraro, R. Maboudian and L. Magagnin, *Surf. Sci. Rep.*, 2007, **62**, 499.
14 Q. Shao, R. H. Que, M. W. Shao, L. Cheng and S. T. Lee, *Adv. Funct. Mater.,* 2012, **22**, 2067.
15 S. Y. Sayed and J. M. Buriak, *ACS Appl. Mater. Interfaces,* 2010, **2**, 3515.
16 E. D. Pailk, *Handbook of Optical Constants of Solids III*, Academic New York, 1998.
17 I. Yoon, T. Kang, W. Choi, J. Kim, Y. Yoo, S. W. Joo, Q. H. Park, H. Ihee and B. Kim, *J. Am. Chem. Soc.*, 2009, **131**, 758.
18 S. M. Wells, I. A. Merkulov, I. I. Kravchenko, N. V. Lavrik and M. J. Sepaniak, *ACS Nano*, 2012, **6**, 2948.
19 M. J. Natan, *Faraday Discuss.*, 2006, **132**, 321.
20 R. H. Que, M. W. Shao, S. J. Zhuo, C. Y. Wen, S. D. Wang and S. T. Lee, *Adv. Funct. Mater.,* 2011, **21**, 3337.
21 D. P. dos Santos, G. F. S. Andrade, M. L. A. Temperini and A. G. Brolo, *J. Phys. Chem. C,* 2009, **113**, 17737.
22 L. Q. Lu, Y. Zheng, W. G. Qu, H. Q. Yu and A. W. Xu, *J. Mater. Chem.*, 2012, **22**, 20986.
23 S. Nakashima and M. Hangyo, *IEEE J. Quantum Electron.*, 1989, **25**, 965.
24 L. Zhang, X. Lang, A. Hirata and M. Chen, *ACS Nano*, 2011, **5**, 4407.
25 Y. Sun and G. P. Wiederrecht, *Small*, 2007, **3**, 1964.
26 T. Wang, Z. S. Zhang, F. Liao, Q. Cai, Y. Q. Li, S. T. Lee and W. M. Shao, *Sci. Rep.*, 2014, **4**, 4052.

Two-step-route to Ag-Au nanoparticles grafted on Ge wafer for extra-uniform SERS substrates

Tao Wang,[a,b] Fei Hu,[a] Emmanuel Ikhile,[c] Fan Liao,[a] Yanqing Li*[a] and Mingwang Shao*[a]

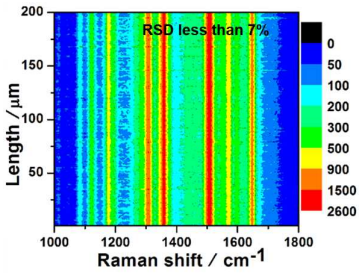

Ag-Au nanoparticles grafted on Ge wafer were fabricated as SERS substrates to detect 200 random spots and obtained the lowest relative standard deviation of less than 7%.